Available online at www.sciencedirect.com

jmr&t Journal of Materials Research and Technology

www.jmrt.com.br

Original Article

Abrasion resistance and toughness of a ductile iron produced by two molding processes with a short austempering

J.R. Dueñas[a], W. Hormaza[b,*], G.M. Castro Güiza[c]

[a] Proyecto Curricular Ingeniería Mecánica, Facultad Tecnológica Universidad Distrital Francisco José de Caldas, Calle 68D Bis A sur # 49F-70, Bogotá, D.C., Colombia

[b] Departamento de Ingeniería Industrial, Universidad de Ingeniería y Tecnología (UTEC), Jr. Medrano Silva 165, Barranco, Lima, Peru

[c] Departamento de Ingeniería Mecánica – Universidad Central, Calle 21 # 4-40, Bogotá, D.C., Colombia

ARTICLE INFO

Article history:
Received 16 August 2018
Accepted 6 February 2019
Available online 27 May 2019

Keywords:
Ausferrite
Cast iron
Impact
Massive carbides
Martensite
Three-body abrasion

ABSTRACT

Austempered ductile irons (ADI) have been extensively used in applications that require a high wear resistance. To further improve it, this work analyzes the effects of both two molding conditions and a short austempering process in the abrasion resistance and toughness of a ductile iron. To do so, the cast and heat-treated specimens were analyzed using several stages including microstructural analysis, mechanical testing and roughness measurements. The experimental results showed that both molding conditions induced the precipitation of massive carbides during solidification, yet the green sand samples had the highest amount. Furthermore, the short austempering produced a microstructure composed by refined ausferrite, with a surrounding mixture of untempered martensite and unreacted austenite. In addition, the ADI presented the best wear resistance due to its hard microstructure which further strengthened during the tests. Finally, the toughness of the ADI was impaired primarily by the mixture of untempered martensite and unreacted austenite.

1. Introduction

Austempered ductile irons (ADI) are a special type of cast iron that is recognized by its combination of strength and toughness and by its outstanding wear resistance in many tribosystems. These remarkable mechanical properties are a consequence of its ausferritic matrix, which is produced by an isothermal heat treatment [1]. During this treatment, ferrite nucleates from graphite nodules and grows as platelets toward the intercellular boundaries [1–3]. Simultaneously, carbon atoms are rejected from the new ferrite platelets toward the surrounding austenite, which becomes stable at room temperature [1–4].

The relationship between the microstructure and the abrasion resistance of ADI has been widely studied in the last years. First of all, Owhadi et al. [5] and Dommarco et al. [6] found that graphite spheroids concentrate wear since they are

* Corresponding author.
E-mail: whormaza@utec.edu.pe (W. Hormaza).

https://doi.org/10.1016/j.jmrt.2019.02.014

easily penetrated by the abrasive. Then, these particles produce deep scratches and comet tails as they leave the nodules. Regarding the matrix microstructure, its effects on wear resistance are closely related to the abrasion conditions. On one hand, Dommarco et al. [6,7] discovered that ausferrite outperforms martensite in moderate to harsh abrasive tribosystems. This behavior is related to the higher toughness of the former, which promotes a microploughing wear mechanism. Moreover, Owhadi et al. [5] showed that a small amount of dispersed unreacted austenite raises the abrasion resistance of ADI, because these loading conditions promote a considerable amount of work hardening, or even strain induced martensitic transformation, on this phase. On the other hand, Dommarco et al. [7] and Yang and Putatunda [8] revealed that hard matrices – like low temperature ausferrite or martensite – perform better in mild tribosystems, where loading is insufficient to produce significant deformation on the abraded surfaces.

In the past two decades, some modifications have been proposed to improve the abrasion resistance of ADI and related ductile irons. For example, Yang and Putatunda [8] introduced a two-step austempering process that increased both mechanical properties and wear resistance in mild abrasive conditions through microstructural refinement. Furthermore, Zhou et al. [9] induced some as quenched martensite and retained austenite to the ausferrite matrix, which raised the impact abrasion resistance of this material. Moreover, Laino et al. [10] introduced Cr alloyed massive carbides to the microstructure of ADI, which enhanced its wear resistance but impaired its impact toughness. Finally, Luo et al. [11] found that a martensitic–austenitic ductile iron surpassed a martensitic ductile iron and a ADI in both pin-on-disk and impact abrasion tests.

In this context, this work will evaluate the wear resistance and impact toughness of a ductile iron subjected to a short austempering and produced by two different molding processes. Furthermore, the obtained materials will be compared against two conventionally treated ductile irons – as cast and quenched and tempered – which had the same chemical composition and were casted with similar molding conditions.

2. Materials and methods

A Mn and Cu alloyed ductile iron (Table 1) that is used in the Colombian industry was melted in a 1-ton induction furnace and was ladle inoculated for 80s using a FeSiMg alloy. Afterwards, the molten metal was poured into green (GS) and CO_2 hardened silicate sand molds (CS) with similar geometry.

Following cooling and demolding, three experimental conditions were studied for each casting process: as cast, austempered and quenched and tempered. All the heat-treated specimens were austenitized at 900 °C for 1 h in an electric resistance furnace. Then, the austempered samples were cooled to 290 °C in a $NaNO_3/KNO_3$ salt bath, where they were hold for 2 min. Meanwhile, the remaining specimens were oil quenched and tempered at 260 °C for 1 h. Finally, both the as cast and heat-treated cast irons were characterized using the techniques described in Table 2.

3. Results and discussion

3.1. *Microstructural analysis*

The ductile iron casted by both molding processes presented well-dispersed graphite spheroids with a similar nodule count (Table 3). However, the nodule size of both molding processes is lower than the ones obtained by Dommarco et al. [6] and Rebasa et al. [12] in similar casting conditions. In addition, the GS samples showed smaller and more irregular nodules than the CS specimens.

Regarding the matrix observed in the as-cast condition, in both molding processes the microstructure consisted of bull's-eye ferrite, fine pearlite and massive carbides (Fig. 1); the latter being identified by EDX analysis as Mn-rich M_3C carbides. Nevertheless, the GS castings presented a lower quantity of ferrite and a larger amount of carbides when compared to CS molds.

With respect to the heat-treated castings, the austempered samples (Figs. 2 and 3) presented a refined ausferrite that nucleated around graphite nodules [1–3], surrounded by a mixture of as quenched lenticular martensite and unreacted austenite, and some sparse M_3C carbides throughout the matrix. In contrast, the quenched and tempered specimens (Fig. 4) showed a microstructure comprising tempered martensite, a small amount of retained austenite and a few M_3C carbides. Lastly, the GS casted samples of both heat-treated conditions presented a higher amount of massive carbides than the CS molded ones.

4. Mechanical properties

4.1. *Bulk hardness and microhardness*

Regarding the molding processes, both the bulk hardness and microhardness (Fig. 5) of the GS nodular iron were higher than the CS ones for all the evaluated conditions. However, there were differences between the trends of bulk hardness and microhardness with respect to the heat treatment process: while the austempered ductile iron presented the highest bulk hardness, the quenched and tempered one showed the maximum microhardness. Finally, the as-cast condition had the lowest values in both mechanical tests

Table 1 – Reported chemical composition of the analyzed ductile iron.

%wt	C	Si	Mn	P	S	Cr	Ni	Cu
Sample	3.38	2.59	0.52	0.019	0.008	0.09	0.03	0.47

Table 2 – Experimental techniques used in this study.

Stage	Technique	Description
Microstructural analysis	Metallographic preparation	Several metallographic samples were prepared from each experimental condition following the ASTM E3 standard. In addition, they were etched with 3% nital (general structure) and 10% sodium metabisulfite (retained austenite) according to the ASTM E407 specification.
	Optical microscopy	A nodularity assessment according to ASTM A247 and a phase analysis were made using an Olympus BX-51M microscope with an Olympus analySIS FIVE image analyzer. Five different images were measured for each experimental condition.
	Scanning electronic microscopy	The morphology and chemical composition of the microconstituents were further studied using a FEI Quanta 200 SEM with an EDX probe.
Mechanical properties	Bulk hardness	The hardness of the as cast samples was measured using a Brinell durometer, according to ASTM E10 standard. In addition, the heat-treated specimens were evaluated by a Rockwell C Hardness test, following the ASTM E18 standard and using a Wilson Rockwell 600 Durometer. For comparison purposes, the latter values were converted to the Brinell scale using the tables shown in the ASTM E140 standard. Each of the reported values is an average of five measurements.
	Microhardness	Vickers microhardness was used with two purposes: to corroborate the information obtained by the bulk hardness tests and to compare the properties of the castings before and after abrasion. All the measurements were made according to ASTM E384 standard using a Buehler MicroMet 5105 microdurometer with a 300 gf load. For all cases, five measurements were averaged.
	Izod impact tests	The toughness of all the samples was assessed by unnotched impact tests using a 150J conventional pendulum, following the ASTM E23 standard. Five different specimens were tested for each condition. Moreover, selected samples were fractographically examined by means of a FEI Quanta 200 SEM.
Abrasion resistance	Dry sand – rubber wheel tests	Several tests were conducted according to the procedure B of the ASTM G65 standard, using a custom-made machine with a NR/SBR rubber wheel (Hardness: 58–62 Shore A) and a AFS 50/70 unground silica sand (U.S. Silica®). The obtained weight loss values were measured on a 0.1 mg precision scale, and then were converted to volume loss. Then, a relative wear resistance index [6] was obtained using an AISI 4340 steel as a reference material. The reported values represent the average from four different tests.
	Surface characterization	Selected worn surfaces were inspected by means of roughness measurements, using a Hommel Tester T1000 apparatus, and microscopical examinations using a FEI Quanta 200 SEM.

Table 3 – Nodularity assessment for both molding processes.

Molding process	Nodule count (Nodules/mm^2)	Nodule diameter (μm)	Nodularity	Nodule type
Green sand	190 ± 3	22 ± 1.6	50%	II-III-V
CO_2 sand	180 ± 2	27 ± 1.7	70%	II-III-V

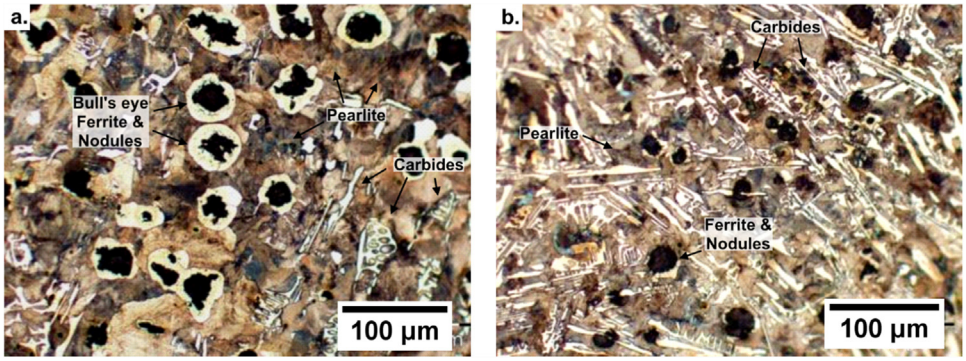

Fig. 1 – Micrographs of the as-cast samples: (a) CO_2 sand molds (CS), (b) green sand molds (GS).

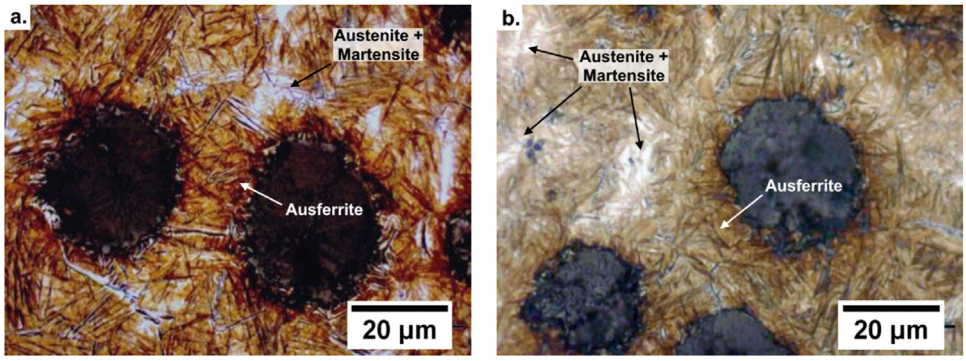

Fig. 2 – Micrographs of the austempered samples (a) CO_2 sand molds (CS), (b) green sand molds (GS).

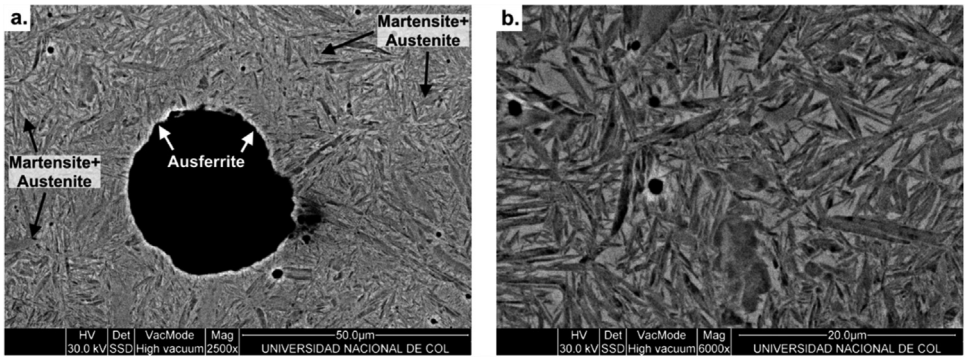

Fig. 3 – SEM micrographs of the austempered samples: (a) distribution of ausferrite and martensite + unreacted austenite zones, (b) detailed view of the lenticular martensite.

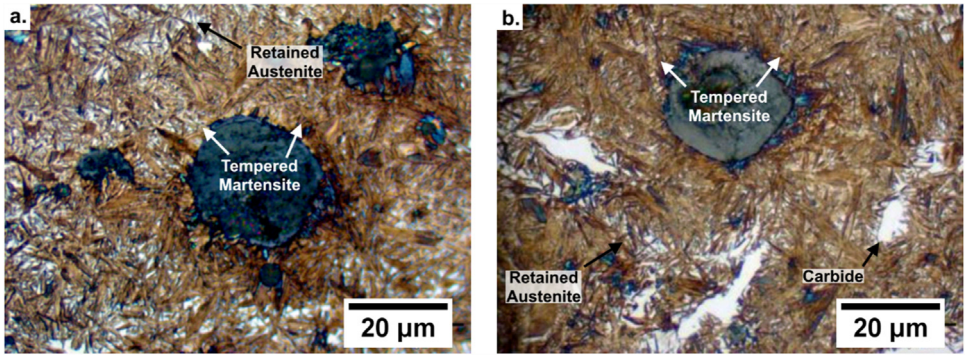

Fig. 4 – Micrographs of the quenched and tempered samples: (a) CO_2 sand molds, (b) green sand molds.

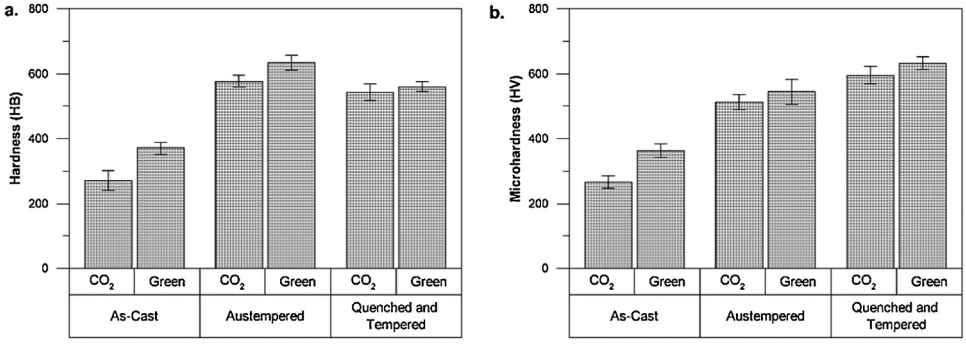

Fig. 5 – Bulk hardness (a) and microhardness (b) of the analyzed samples. Error bars are a 95% confidence interval.

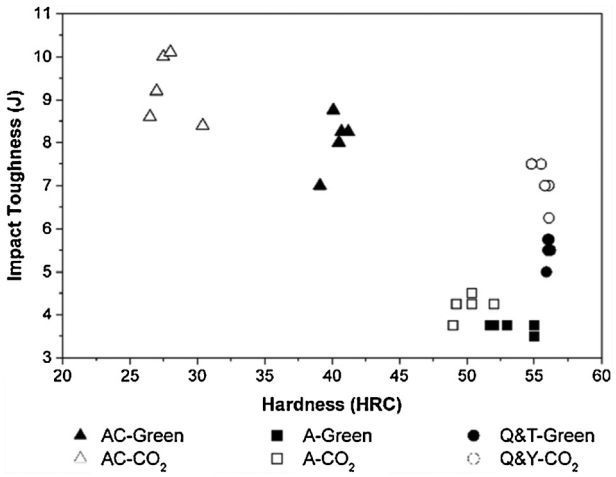

Fig. 6 – Impact test results (AC: As cast, A: Austempered, Q&T: Quenched and tempered).

4.2. *Impact tests*

The impact tests (Fig. 6) of the analyzed samples showed that the austempering process greatly impaired the toughness of the cast iron, when compared with the as-cast and quenched and tempered conditions. As to the effect of the molding process, the CS castings were consistently tougher than the GS ones regardless of the experimental condition.

The fracture surfaces of the as cast samples (Fig. 7) revealed a cleavage mechanism for both molding conditions. However, the GS specimens presented bigger and flatter cleavage facets, which have been observed in ductile irons with a significant amount of massive carbides [13]. In contrast, the fracture surface of the austempered castings (Fig. 8) showed a mixed mechanism comprising quasicleavage with a few microvoids in the regions next to the graphite nodules, and flat fractures in some of the intercellular spaces. These regions can be associated with the detachment of the mixture of untempered martensite and unreacted austenite. Finally, the quenched and tempered specimens (Fig. 9) exhibited an irregular fracture surface with a mixed failure mode, comprising microvoids and cleavage mechanisms. In addition, the nodular cavities exhibited a significant deformation, which indicates a ductile behavior [13] and agrees with the higher toughness obtained in these samples, when compared to the austempered ones.

4.3. *Abrasion wear tests*

The abrasion wear tests (Fig. 10) revealed that the austempered ductile iron had the highest relative wear resistance, followed by the as-cast and the quenched and tempered conditions. Besides, the GS samples presented better relative wear resistance than the CS specimens, regardless of the applied heat treatment.

The microexamination of the worn surfaces (Fig. 11) showed that the austempered samples presented the narrower wear trails, when compared to as-cast or quenched and tempered specimens. Furthermore, the surface of the as-cast samples presented a high number of small, irregular pits, which were less frequent in both heat-treated conditions.

The mean roughness of the worn surfaces (Fig. 12) was higher for the GS molds in all the experimental conditions.

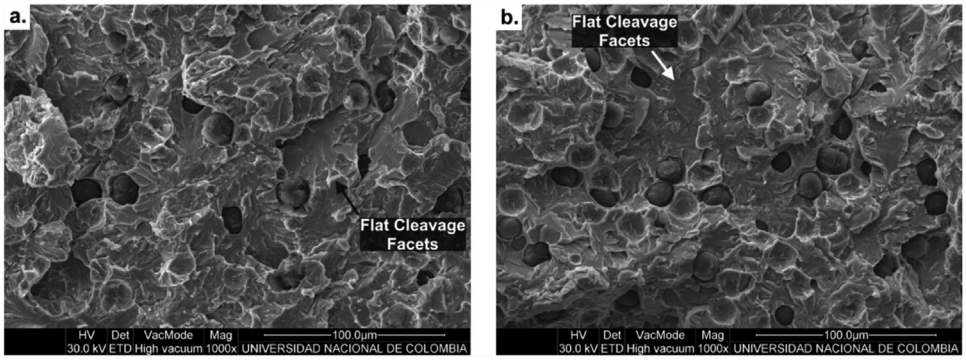

Fig. 7 – Fracture surfaces of the as-cast samples: (a) CO_2 sand (CS) molds, (b) green sand (GS) molds.

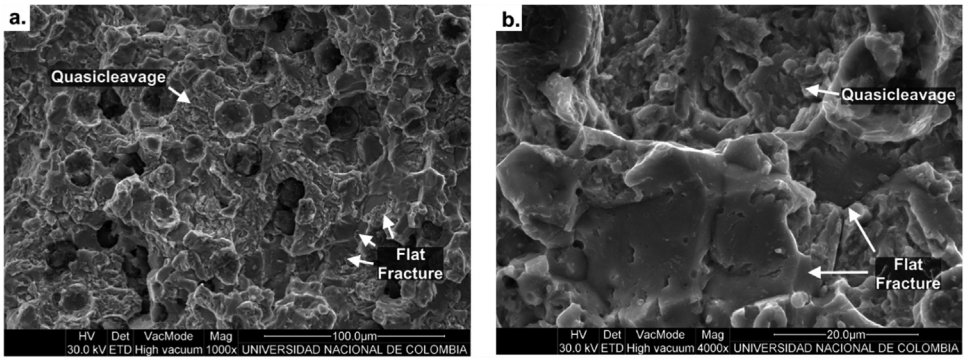

Fig. 8 – Fracture surfaces of the austempered samples: (a) general view, (b) detailed morphology.

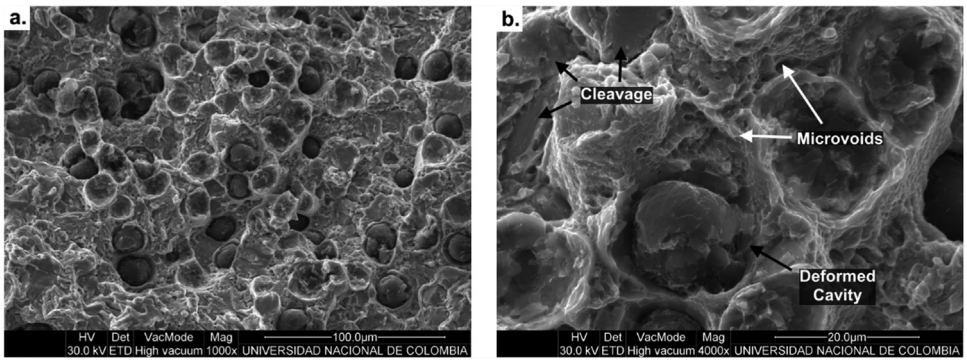

Fig. 9 – Fracture surfaces of the quenched and tempered samples: (a) general view, (b) detailed morphology.

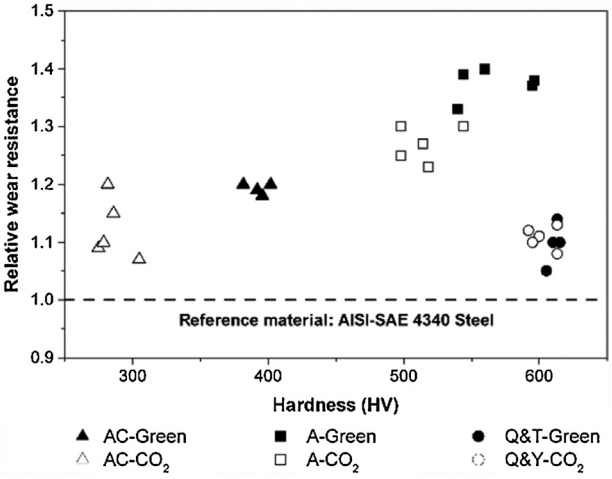

Fig. 10 – Wear resistance of the as cast (AC), austempered (A) and quenched and tempered (Q&T) samples.

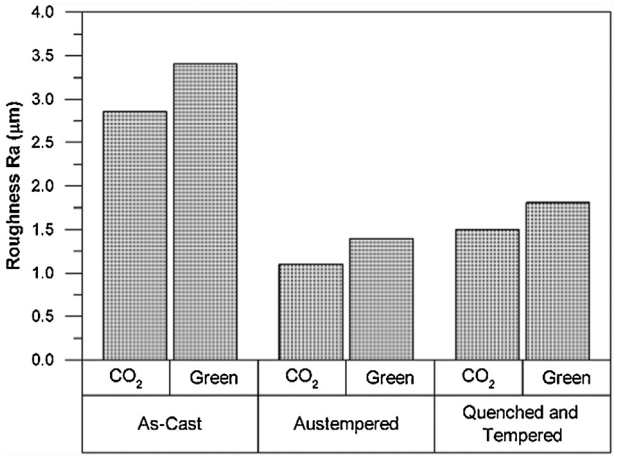

Fig. 12 – Mean roughness values (Ra) of the worn surfaces.

Additionally, the roughness of the as cast samples was higher than the one found on the heat-treated samples. This correlates well with the pitted surface that was observed in the microexamination of those specimens. Regarding the heat-treated samples, the austempered condition presented the lowest roughness, which agrees with its superior wear resistance when compared to the quenched and tempered specimens.

The microhardness measurements made on both the worn and unaffected surfaces (Fig. 13) revealed a significant hardening of the austempered samples. In contrast, neither the as cast nor the quenched and tempered samples presented a considerable change in their hardness after the abrasion test.

5. Discussion

The experimental results showed that both the molding process and the applied heat treatment affected the mechanical properties of the ductile iron. First, the better thermal conductivity of the GS molds induced a higher supercooling in the molten metal, thus increasing the amount of massive

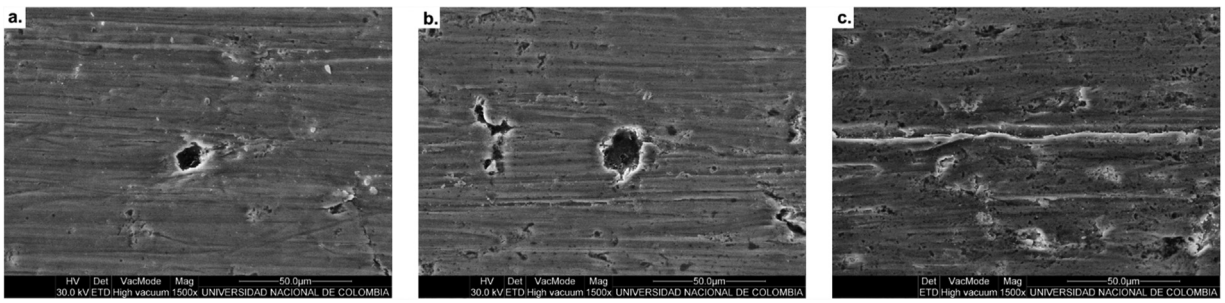

Fig. 11 – Worn surfaces of the (a) austempered, (b) quenched and tempered and (c) as-cast samples.

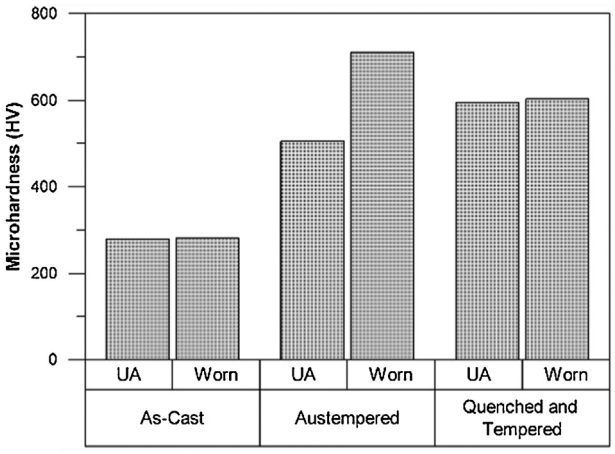

Fig. 13 – Microhardness measurements on the unaffected (UA) and worn surfaces.

carbides and reducing the quantity of bull's eye ferrite and the mean nodule diameter of these castings [14,15]. Furthermore, the significant amount of Mn in the chemical composition of the molten metal further promoted the precipitation of carbides during the solidification in both molding conditions [16].

During the austempering process, the matrix microstructure evolved in the following way: first, ausferrite nucleated on the graphite nodules and grew toward the intercellular boundaries. However, the austempering time was not enough to complete the transformation, thus leaving a significant amount of unstable austenite in the intercellular borders. Then, this phase partially transformed to untempered martensite at the end of the heat treatment. This microstructure agrees with the findings made by Owhardi et al. [5], whose work studied the microstructural and mechanical properties of a 1.5% Mn ADI treated from 5 min to 48 h. However, the ausferrite formation kinetics of the alloy analyzed in this work are expected to be faster than the one experienced by the 1.5% Mn ADI, given the differences both in the Mn and Si contents and in the austempering temperature between the two studies.

Regarding the hardness and microhardness measurements, the experimental results were contradictory since the austempered samples presented the highest bulk hardness, while the quenched and tempered specimens showed the maximum microhardness. This difference can be explained by the response of the unreacted austenite to the test conditions. On one hand, the bulk hardness uses a high load that produces considerable strain hardening, or even strain induced martensitic transformation, around the indentations. On the other hand, the low load that is employed in the microhardness tests is not enough to produce the same amount of plastic deformation on the surface of the material, thus inducing less strain hardening. This behavior has been widely reported during abrasion tests of ADI [5–8].

The impact toughness of the austempered samples was considerably impaired by the mixture of untempered martensite and unreacted austenite that was present in the intercellular boundaries. This microconstituent provided a preferential fracture path, as observed in the fractographs of the austempered samples, which was responsible for the reduced impact energy. This has been reported in similar microstructures by Owhadi et al. [5] and Zhou et al. [9]. However, when austempered ductile irons are compared to other wear resistant materials – like white cast irons – they offer a better compromise between impact toughness and abrasion resistance. Concerning the effect of the molding process, all the GS samples presented a lower toughness than the CS ones. This was more evident for the as-cast samples, as demonstrated by the morphology of their fracture surfaces, but also affected the quenched and tempered ones. Basso et al. [17] demonstrated that the presence of massive carbides on ductile iron matrices impairs their toughness since those particles serve as a preferential fracture path. However, the effect of the mixture of untempered martensite and unreacted austenite was more significant than the one from the massive carbides in the austempered samples.

Finally, the better wear resistance of the austempered samples with respect to the other experimental conditions was related to two factors: the high initial hardness that was produced by the mixed microstructure; and the work hardening ability of the unreacted austenite, which is apparent when comparing the hardness of the worn surfaces before and after the abrasion test. Both factors induced a lower abrasive penetration on the austempered surface that explains the high wear resistance observed in the analyzed samples. Moreover, similar microstructures have also presented a comparable behavior when submitted to abrasive [5] or impact wear conditions [9].

Regarding the effect of the molding process, the presence of a higher amount of massive carbides in the GS samples clearly improved their abrasion resistance, especially for the as-cast condition. This effect was previously reported by Laino et al. [18], who stated that carbides enhance the wear resistance of ductile irons in mild tribosystems that produce small scratches. Furthermore, the small pits found on the as-cast samples can be related to carbide fracture and pull-out, which is characteristic of carbidic ductile irons subjected to mild abrasive conditions [18].

6. Conclusions

From the experimental results, it was possible to conclude that the short austempering process produced a superior wear resistance than the quenched and tempered or the as-cast conditions for the studied ductile iron. This was caused by the mixture of ausferrite, untempered martensite and unreacted austenite, which simultaneously provided a high initial hardness and a significant work hardening capacity. Nevertheless, the impact toughness was impaired by the austempering process, since the intercellular regions provided a preferential path for fracture propagation. Finally, the higher amount of carbides produced by the green sand molding process improved the abrasion resistance of all experimental conditions, but simultaneously reduced the impact toughness of the as-cast and quenched and tempered samples. This last effect was not significant in the austempered condition due to the brittle nature of the matrix.

Funding

This research did not receive any specific grant from funding agencies in the public, commercial, or not-for-profit sectors.

Conflicts of interest

The authors declare no conflicts of interest.

REFERENCES

[1] Tanaka Y, Kage H. Development and application of austempered spheroidal graphite cast iron. Mater Trans JIM 1992;33:543–57, http://dx.doi.org/10.2320/matertrans1989.33.543.
[2] Pourasiabi H, Saghafian H, Pourasiabi H. Effect of austempering process on microstructure and wear behavior of ductile iron containing Mn—Ni—Cu—Mo. Met Mater Int 2013;19:67–76, http://dx.doi.org/10.1007/s12540-013-0030-9.
[3] Pérez MJ, Cisneros M, López HF. Wear resistance of Cu—Ni—Mo austempered ductile iron. Wear 2006;260:879–85, http://dx.doi.org/10.1016/j.wear.2005.04.001.
[4] Shepperson S, Allen C. The abrasive wear behaviour of austempered spheroidal cast irons. Wear 1988;121:271–87, http://dx.doi.org/10.1016/0043-1648(88)90206-2.
[5] Owhadi A, Hedjazi J, Davami P. Wear behaviour of 1.5Mn austempered ductile iron. Mater Sci Technol 1998;14:245–50, http://dx.doi.org/10.1179/mst.1998.14.3.245.
[6] Dommarco RC, Sousa ME, Sikora JA. Abrasion resistance of high nodule count ductile iron with different matrix microstructures. Wear 2004;257:1185–92, http://dx.doi.org/10.1016/j.wear.2004.08.002.
[7] Dommarco R, Galarreta I, Ortız H, David P, Maglieri G. The use of ductile iron for wheel loader bucket tips. Wear 2001;249:100–7, http://dx.doi.org/10.1016/S0043-1648(01)00531-2.
[8] Yang J, Putatunda SK. Effect of microstructure on abrasion wear behavior of austempered ductile cast iron (ADI) processed by a novel two-step austempering process. Mater Sci Eng A 2005;406:217–28, http://dx.doi.org/10.1016/j.msea.2005.06.036.
[9] Zhou R, Jiang Y, Lu D, Zhou R, Li Z. Development and characterization of a wear resistant bainite/martensite ductile iron by combination of alloying and a controlled cooling heat-treatment. Wear 2001;250:529–34, http://dx.doi.org/10.1016/S0043-1648(01)00603-2.
[10] Laino S, Sikora JA, Dommarco RC. Development of wear resistant carbidic austempered ductile iron (CADI). Wear 2008;265:1–7, http://dx.doi.org/10.1016/j.wear.2007.08.013.
[11] Luo Q, Xie J, Song Y. Effects of microstructures on the abrasive wear behaviour of spheroidal cast iron. Wear 1995;184:1–10, http://dx.doi.org/10.1016/0043-1648(94)06499-7.
[12] Rebasa N, Dommarco R, Sikora J. Wear resistance of high nodule count ductile iron. Wear 2002;253:855–61, http://dx.doi.org/10.1016/S0043-1648(02)00171-0.
[13] Refaey A, Fatahalla N. Effect of microstructure on properties of ADI and low alloyed ductile iron. J Mater Sci 2003;38:351–62, http://dx.doi.org/10.1023/A:1021177902596.
[14] Giacopini A, Boeri RE, Sikora JA. Carbide dissolution in thin wall ductile iron. Mater Sci Technol 2003;19:1755–60, http://dx.doi.org/10.1179/026708303225009445.
[15] Ceccarelli B, Dommarco R, Martınez R, Martınez Gamba M. Abrasion and impact properties of partially chilled ductile iron. Wear 2004;256:49–55, http://dx.doi.org/10.1016/S0043-1648(03)00257-6.
[16] Davis JR. ASM specialty handbook: cast irons. ASM International; 1996.
[17] Basso A, Laino S, Dommarco RC. Wear behavior of carbidic ductile iron with different matrices and carbide distribution. Tribol Trans 2013;56:33–40, http://dx.doi.org/10.1080/10402004.2012.725149.
[18] Laino S, Sikora JA, Dommarco RC. Influence of chemical composition and solidification rate on the abrasion and impact properties of CADI. ISIJ Int 2009;49:1239–45, http://dx.doi.org/10.2355/isijinternational.49.1239.